Journal of Controlled Release 292 (2018) 163–171

Contents lists available at ScienceDirect

Journal of Controlled Release

journal homepage: www.elsevier.com/locate/jconrel

Boosting RNAi therapy for orthotopic glioblastoma with nontoxic brain-targeting chimaeric polymersomes

Yanan Shi, Yu Jiang, Jinsong Cao, Weijing Yang, Jian Zhang*, Fenghua Meng, Zhiyuan Zhong*

Biomedical Polymers Laboratory, College of Chemistry, Chemical Engineering and Materials Science, State Key Laboratory of Radiation Medicine and Protection, Soochow University, Suzhou 215123, PR China

ARTICLE INFO

Keywords:
Blood brain barrier
Glioblastoma
Gene delivery
siRNA
Targeted delivery

ABSTRACT

Glioblastoma with intracranial infiltrative growth remains an incurable disease mainly owing to existence of blood brain barrier (BBB) and off-target drug toxicity. RNA interference (RNAi) with a high specificity and low toxicity emerges as a new treatment modality for glioblastoma. The clinical application of RNAi technology is, however, hampered by the absence of safe and brain-targeting transfection agents. Here, we report on angiopep-2 peptide-decorated chimaeric polymersomes (ANG-CP) as a nontoxic and brain-targeting non-viral vector to boost the RNAi therapy for human glioblastoma *in vivo*. ANG-CP shows excellent packaging and protection of anti-PLK1 siRNA (siPLK1) in its lumen while quickly releasing payloads in a cytoplasmic reductive environment. Notably, *in vitro* experiments demonstrate that ANG-CP can effectively permeate the bEnd.3 monolayer, transport siRNA into the cytosol of U-87 MG glioblastoma cells *via* the LRP-1-mediated pathway, and significantly silence PLK1 mRNA and corresponding oncoprotein in U-87 MG cells. ANG-CP greatly prolongs the siPLK1 circulation time and enhances its accumulation in glioblastoma. RNAi with siPLK1 induces a strong anti-glioblastoma effect and significantly improves the survival time of glioblastoma carrying mice.

1. Introduction

Glioblastoma with intracranial infiltrative growth remains an incurable disease. One of the reasons is the poor permeability of therapeutics through the blood brain barrier (BBB) [1–4]. In the past years, brain-targeting nanomedicines that are able to cross the BBB have been designed to enhance the chemotherapy for glioblastoma *in vivo* [5–8]. Low-density lipoprotein receptor-related protein-1 (LRP-1), over-expressed on both BBB and glioblastoma cells, has emerged as a particularly appealing target for glioblastoma therapy [9,10]. Angiopep-2 peptide has shown a high selectivity to LRP-1 [11–15]. Currently, two ANG-drug conjugates are clinically tested [16,17]. Work from different groups reveals that the use of ANG ligands in nanotherapeutics greatly enhances their BBB permeation, leading to strongly improved chemotherapy for glioblastoma *in vivo* [18,19]. The high off-target toxicity of chemotherapeutics, even after encapsulation in nanosystems, however, lends it unattractive for clinical translation.

RNA interference (RNAi) with a high specificity and low toxicity emerges as a new treatment modality for cancers including glioblastoma [20–24]. Unlike chemotherapeutics, RNAi is used to treat cancer *via* silencing carcinogenic genes at the mRNA level [25]. Several small interfering RNAs (siRNAs), targeting oncogenes like polo-like kinase 1 (PLK1) [26,27], epithelial growth factor receptor (EGFR) [28,29] or B-cell lymphoma 2 like protein 12 (Bcl2L12) [30], have been reported to effectively suppress the growth of glioblastoma cells. Recently, Chen et al. reported that lipoprotein-biomimetic nanosystems mediate targeted delivery of siRNA to glioblastoma cells through macropinocytosis [31]. Notably, most RNAi therapy reported for orthotopic glioblastoma was based on cationic polymers or lipid nanoparticles through local delivery, due to possible stimulation of the immune system [26,32,33]. The development of translatable, safe and brain-targeting transfection agents is the key to the clinical success of RNAi therapy for glioblastoma.

Here, we report on the design of ANG-decorated chimaeric polymersomes (ANG-CP) as a nontoxic and brain-targeting non-viral vector to boost RNAi therapy for human glioblastoma *in vivo* (Scheme 1). Our earlier work has shown that cNGQ peptide-functionalized chimaeric polymersomes based on poly(ethylene glycol)-b-poly(trimethylene carbonate-*co*-dithiolane trimethylene carbonate)-b-polyethylenimine copolymers mimicking viruses mediate efficient transfection in orthotopically xenografted human lung tumors [34]. Intriguingly, *in vitro* and *in vivo* experiments reveal that siRNA against firefly luciferase (siGL3) and siPLK1-loaded ANG-CP can cross the BBB, actively target U-87 MG glioblastoma cells, and release siRNA into the cytoplasm. Furthermore,

* Corresponding authors.
E-mail addresses: jianzhangsd@suda.edu.cn (J. Zhang), zyzhong@suda.edu.cn (Z. Zhong).

https://doi.org/10.1016/j.jconrel.2018.10.034
Received 4 September 2018; Received in revised form 20 October 2018; Accepted 30 October 2018
Available online 05 November 2018
0168-3659/

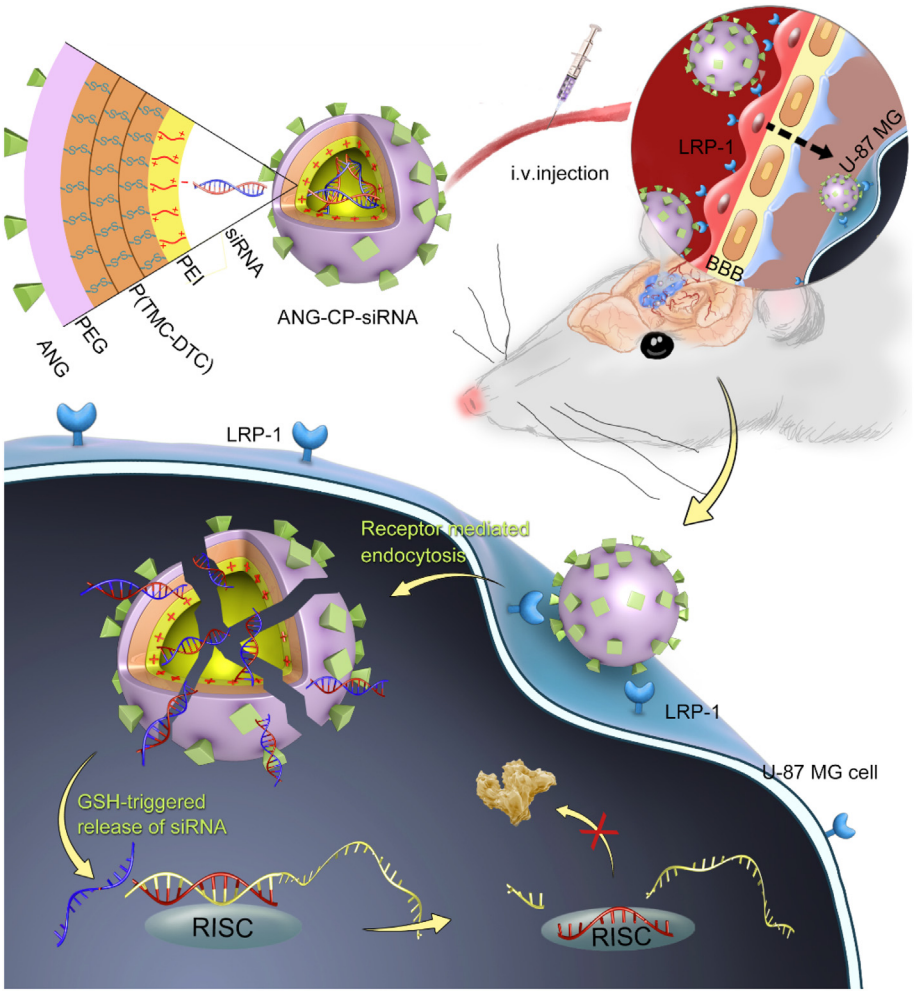

Scheme 1. Illustration of improved RNAi therapy for human glioblastoma *in vivo* using siRNA-loaded nontoxic brain-targeting chimaeric polymersomes (ANG-CP-siRNA). ANG-CP-siRNA can efficiently load and protect siRNA from degradation, cross BBB and target to U-87 MG glioblastoma cells *via* an LRP-1 mediated mechanism, and quickly release siRNA into the cytoplasm of glioblastoma cells, resulting in highly efficient treatment of glioblastoma. In the cytoplasm, there exists a high reducing potential which would not only trigger polymersome decrosslinking by cleaving the disulfide crosslinks but also increase the hydrophilicity of the polymersomal membrane, resulting in polymersome dissociation and fast cytoplasmic siRNA release.

RNAi with siPLK1-loaded ANG-CP induces a potent anti-glioblastoma effect and significantly improves the survival time of mice with an orthotopic human glioblastoma. The high RNAi potency and excellent safety render these brain-targeting chimaeric polymersomes highly appealing for glioblastoma therapy.

2. Materials and methods

2.1. Glutathione (GSH)-triggered siRNA release

The procedures of polymer synthesis and preparation of ANG-CP-siRNA were described in detail in Supplementary Data. The GSH-triggered siRNA release profiles of ANG-CP were evaluated by a gel retardation assay. Briefly, gel electrophoresis was carried out using 1% (w/v) agarose gel in Tris/Boric acid/EDTA (TBE, 1 ×) buffer with 3 μL of GelRed for siRNA staining. Free siRNA, ANG-CP-siScramble, CP-siPLK1 or ANG-CP-siPLK1 in 20 μL of PB (5 mM, pH 7.4) at an siRNA concentration of 0.056 μg/μL were incubated with or without 10 mM GSH at 25 °C overnight. After that, the samples were added to separate wells of agarose gel and electrophoresed at 100 V for 30 min. After electrophoresis, gel images were recorded using a Molecular Imager FX (Bio-Rad, Hercules, CA) (Ex/Em: 532/605 nm) and analyzed using Quantity One software (Bio-Rad).

2.2. In vitro BBB transcytosis

The LRP-1 mediated BBB transcytosis capability of ANG-CP was evaluated on an *in vitro* BBB model formed by a bEnd.3 monolayer cultured in 24-well plates (cell-free lower chamber, filled with 800 μL of culture medium) equipped with transwell inserts (monolayer-growth upper chamber, filled with 300 μL of culture medium) (Corning, USA) [35]. In brief, bEnd.3 cells were cultured in Dulbecco modified eagle medium (DMEM) containing 10% fetal bovine serum (FBS) and seeded on the upper chamber at a density of 5×10^4 cells/well for monolayer formation. The bEnd.3 monolayer with a trans-endothelial electrical resistance (TEER) above 200 Ω·cm^2 was then used for transwell measurements of ANG-CP [36]. To eliminate the contribution of non-specific paracellular permeability of the monolayer, an efflux ratio assay (defined as the ratio between the apical-to-basolateral and the basolateral-to-apical permeability, indicating the active transport of ANG-CP by LRP-1 from blood to brain parenchyma) was used (Fig. S1). siScramble(Cy5) was loaded into polymersomes and quantified *via* fluorescence spectrophotometer (Thermo Scientific, USA). For the efflux ratio assay, siScramble(Cy5) loaded ANG-CP (ANG-CP-siScramble (Cy5)) with a final siScramble(Cy5) concentration of 1 μM in upper or lower chamber was incubated in a shaking bath (50 rpm) at 37 °C. Samples at either side of the bEnd.3 monolayer (300 μL from apical chamber or 800 μL from basolateral chamber) were collected at 6 h, 12 h and 24 h, and replaced with an equal volume of fresh medium, and then quantified by fluorescence spectrophotometer.

2.3. In vitro gene silencing

The *in vitro* gene silencing capability of siRNA loaded ANG-CP was studied using U-87 MG-Luc cells and siGL3 as a model siRNA. In brief, U-87 MG-Luc cells were seeded in 96-well plates at a density of 5×10^3

cells/well for 24 h. Then, 90 μL of fresh medium and ANG-CP-siGL3 suspended in 10 μL of PBS was added to give a final siRNA concentration of 200 nM or 400 nM. Cells without ANG-CP-siGL3 treatment were used as control. After 48 h incubation, the cells were lysed using the cell lysis buffer (Beyotime Biotechnology, China) and the luciferase activity was determined using a fluorescent microplate reader (Mithras LB 940, Berthold technologies, Germany). The gene silencing efficacy of ANG-CP-siGL3 for luciferase reporter gene was calculated by comparing the luciferase activities of ANG-CP-siGL3 treated group to that of control group. All the samples were prepared in quadruplicate. Furthermore, the cellular level of PLK1 mRNA was evaluated using quantitative reverse transcription polymerase chain reaction (qRT-PCR) [37]. U-87 MG cells were seeded into 6-well plates (3×10^5 cells/well) and incubated for 24 h. ANG-CP-siPLK1 was added at a final siPLK1 concentration of 200 nM or 400 nM and further incubated for 4 h. The siRNA containing culture medium was replaced with an equal volume of fresh medium, followed by further incubation of the cells for 44 h. Subsequently, the transfected U-87 MG cells were collected and total RNA was isolated using total RNA isolation reagent (Biosharp, China) according to the protocol of manufacturer and tested by qPCR (Bio-Rad, USA). Data are expressed as the fold changes in PLK1 expression relative to the untreated control cells and normalized with the housekeeping gene glyceraldehydes phosphate dehydrogenase (GAPDH) as the endogenous reference. The mRNA expression levels were calculated from the $2^{-\Delta\Delta CT}$ method, and each sample was divided into four groups, taking the mean final result and the standard deviation. The oligodeoxynucleotide primers used for PCR amplification were PLK1-fw: 5′-CGA CTT CGT GTT CGT GGT G-3′, PLK1-rev: 5′-CCC GTC ATA TTC GAC TTT GGT-3′, GAPDH-fw: 5′-CAT GAG AAG TAT GAC AAC AGC CT-3′, GAPDH-rev: 5′-AGT CCT TCC ACG ATA CCA AAG T-3′. For Western blot assay [38], U-87 MG cells were lysed with radio-immuno-precipitation buffer (Beyotime Institute of Biotechnology, China) supplemented with protease and phosphatase inhibitors (Beyotime Institute of Biotechnology). The protein concentration was determined using BCA Protein Assay Kit (Pierce, USA). Protein (30–50 μg) was separated by sodium dodecyl sulfate-polyacrylamide gel electrophoresis on a 10–12% gel and transferred to a polyvinylidene difluoride membrane (Millipore, USA) that was blocked with 5% bovine serum albumin (BSA) for 1 h at room temperature and then probed overnight at 4 °C with rabbit PLK1 antibody (CST, USA). The membrane was washed with Tris-buffered saline/0.1% Tween-20 followed by incubation with secondary antibody. GAPDH (Sigma-Aldrich, China) was used as endogenous control. The Blots were analyzed with the Quantity One software (Bio-Rad Laboratories, USA).

2.4. Pharmacokinetics

siPLK1(Cy5) was used for studying the pharmacokinetics at a siPLK1(Cy5) dosage of 1 mg/kg. Free siPLK1(Cy5), CP-siPLK1(Cy5) and ANG-CP-siPLK1(Cy5) were administered to BALB/c athymic nude mice *via* the tail vein, respectively. At preset time points post-administration, 50 μL of blood sample was withdrawn from the orbital of animal and centrifuged at 3000 rpm for 5 min immediately. The supernatant was then added to 700 μL of DMSO (containing 40 mM dithiothreitol (DTT) for reduction-triggered polymersomal destabilization) and extracted at 37 °C overnight, followed by another centrifugation of 1.5×10^4 rpm × 30 min. The Cy5 content in the supernatant was quantified by fluorometry using Cary Eclipse fluorospectrophotometer (Agilent Technology, USA).

2.5. Orthotopic glioblastoma targeted accumulation of ANG-CP-siPLK1(Cy5)

Orthotopic U-87 MG-Luc glioblastoma bearing female BALB/c nude mice were i.p. injected with $_D$-Luciferin potassium salt, the substrate for firefly luciferase, at a dose of 75 mg/kg for bioluminescence. Animals with similar glioblastoma burden were then randomly divided into two groups ($n = 3$) and i.v. injected with either CP-siPLK1(Cy5) or ANG-CP-siPLK1(Cy5) at siPLK1(Cy5) dosage of 1 mg/kg. At 2, 4, 8, 12 and 24 h post-injection, the mice were anesthetized with pentobarbital sodium (80 mg/kg), and whole body fluorescence images were acquired using a near-infrared fluorescence imaging system (Caliper IVIS Lumina II, Ex 640 nm, Em 668 nm). Mice were sacrificed at 24 h post-injection and the intracranial tumors were taken out for *ex vivo* imaging and region of interest (ROI) analysis using the Lumina II software. The signal intensity was quantified as the flux of all detected photon counts within a constant area.

2.6. In vivo gene silencing

The *in vivo* firefly luciferase gene silencing efficacy of ANG-CP-siGL3 was also evaluated by *in vivo* near-infrared fluorescence imaging. Animals with similar glioblastoma burden were injected with ANG-CP-siGL3, CP-siGL3 or ANG-CP-siScramble at siRNA dose of 60 μg/mouse. Bioluminescence images were taken at 0 h, 24 h and 48 h post-injection. ROI analysis was also carried out for bioluminescence images. Mice treated with PBS were used as control.

2.7. In vivo anti-glioblastoma efficacy

On day 10 post tumor implantation, orthotopic U-87 MG-Luc glioblastoma bearing BALB/c nude mice were imaged *via* bioluminescence. Animals with similar tumor burden were randomly divided into 4 groups ($n = 8$) and i.v. injected with either ANG-CP-siPLK1, CP-siPLK1, ANG-CP-siScrambe or PBS (as control) at siRNA dose of 60 μg/mouse on day 10, 12, 14, 16 and 18 post-implantation (The day of tumor implantation was designated as day 0). The tumor progression was monitored by bioluminescence imaging on day 14, 18 and 22 using the Lumina IVIS II system. Mice were weighed and normalized to their initial weights. The survival of animals was recorded throughout the treatment. In addition, a representative mouse of each group was sacrificed and main organs including tumor, liver, heart, spleen, lung and kidney were excised on day 20. The tissues were fixed with 4% formalin solution and embedded in paraffin. The sliced organ tissues (thickness: 4 μm) mounted on glass slides were stained by hematoxylin and eosin (H&E) and observed with a digital microscope (Leica QWin, Germany).

2.8. Statistical analysis

All data are presented as the mean ± standard deviation (SD). One-way analysis of variance (ANOVA) was used to determine significance among groups, after which post-hoc tests with the Bonferroni correction were used for comparison between individual groups. Statistical significance was established at $^*p < 0.05$, $^{**}p < 0.01$ and $^{***}p < 0.001$.

3. Results and discussion

3.1. Preparation of ANG-CP-siPLK1

ANG-functionalized poly(ethylene glycol)-*b*-poly(trimethylene carbonate-co-dithiolane trimethylene carbonate) (ANG-PEG-P(TMC-co-DTC)) was obtained by conjugating ANG with a cysteine on C-terminal (sequence: TFFYGGSRGKRNNFKTEEYC) to maleimide-functionalized PEG-P(TMC-co-DTC). ANG-CP-siPLK1 was easily fabricated by mixing a solution (100 μL) of poly(ethylene glycol)-*b*-poly(trimethylene carbonate-*co*-dithiolane trimethylene carbonate)-*b*-polyethylenimine (PEG-P(TMC-co-DTC)-PEI) and ANG-PEG-P(TMC-co-DTC) (80/20, mol/mol) in DMSO and a solution (100 μL) of a predetermined amount of siPLK1 in diethyl pyrocarbonate (DEPC)-treated water, followed by injection into 800 μL of HEPES buffer (pH 6.8) and dialysis against HEPES buffer. ANG-PEG-P(TMC-co-DTC) had a longer PEG spacer (M_n = 7.5 kg/mol)

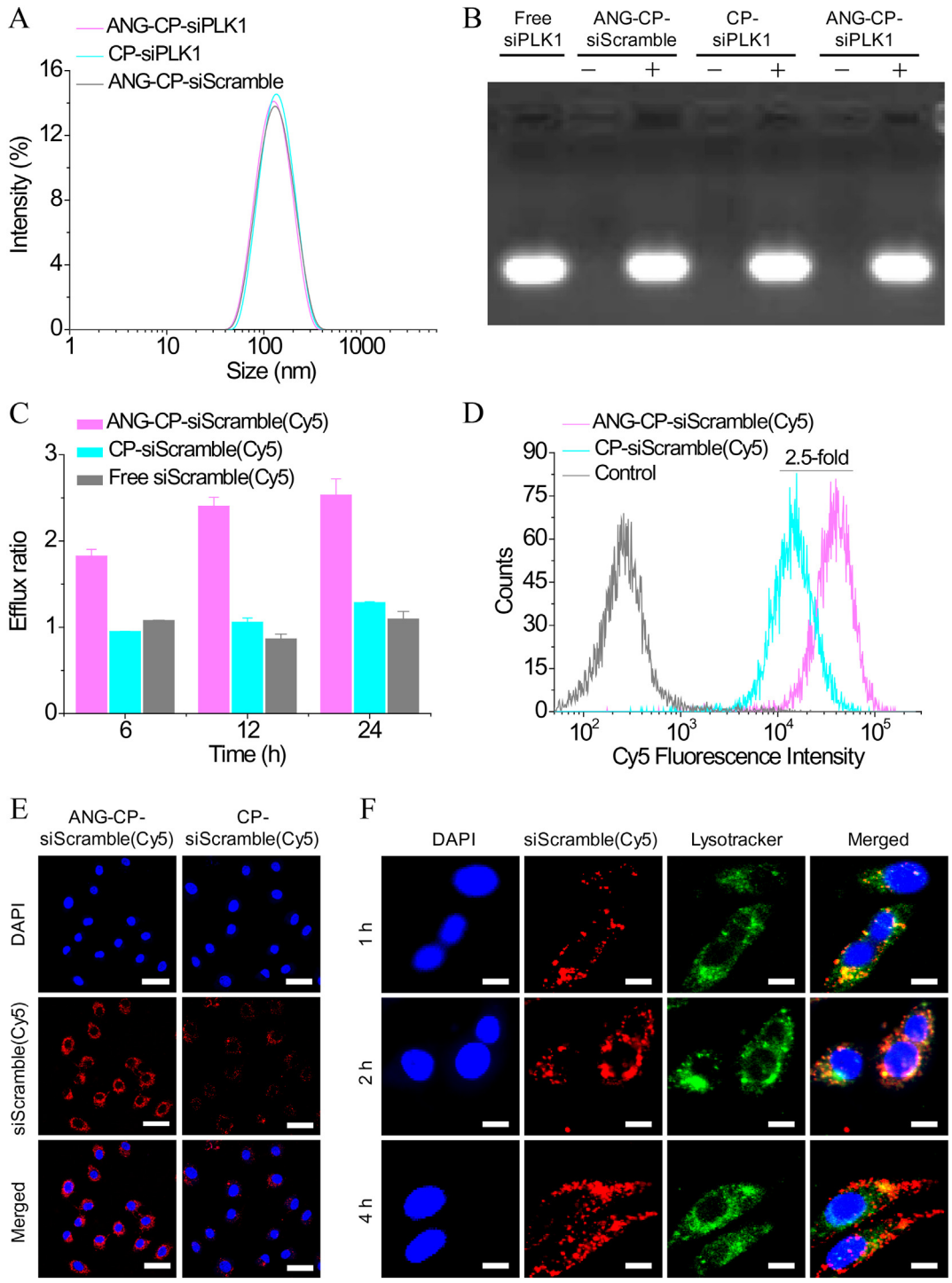

Fig. 1. A) Size distribution of ANG-CP-siPLK1, CP-siPLK1 and ANG-CP-siScramble, determined by DLS; B) Gel retardation assays of ANG-CP-siPLK1, CP-siPLK1 and ANG-CP-siScramble with (+) or without (−) 10 mM GSH treatment overnight. Free siPLK1 was used as a control; C) Efflux ratios of ANG-CP-siScramble(Cy5), CP-siScramble(Cy5) and siScramble(Cy5) for a bEnd.3 monolayer simulating the BBB; D) Flow cytometry of U-87 MG cells following 4 h incubation with either ANG-CP-siScramble(Cy5) or CP-siScramble(Cy5) (siRNA dosage: 200 nM); E) Confocal laser scanning microscopy (CLSM) images of U-87 MG cells following transfection with ANG-CP-siScramble(Cy5) or CP-siScramble(Cy5) (siRNA dosage: 200 nM); F) CLSM images of U-87 MG cells following transfection with ANG-CP-siScramble(Cy5) (siRNA dosage: 200 nM). For each panel, the images from left to the right were cell nuclei stained by DAPI (blue), lysosomes stained by lysotracker red (green), siScramble(Cy5) (red), and overlays of the three images. Bar: 20 μm. (For interpretation of the references to colour in this figure legend, the reader is referred to the web version of this article.)

compared with PEG-P(TMC-co-DTC)-PEI (M_n = 5.0 kg/mol) for effective exposure of the ANG ligand. Interestingly, at a designed siPLK1 loading of 10 wt%, ANG-CP showed excellent encapsulation efficiency of 94.5% and siPLK1 loading content of 9.6 wt%, corresponding to an N/P ratio of 4.0 (Table S1). In contrast, a high N/P ratio of 10–100 is typically needed for non-crosslinked cationic polymers to achieve effective siRNA binding or condensation [39–41]. ANG-CP-siPLK1 had a relatively small size of 115 ± 1.9 nm, as revealed by dynamic light scattering (DLS) (Fig. 1A), and a neutral zeta potential of +0.4 mV (Table S1). We have also prepared a non-targeted control and placebo,

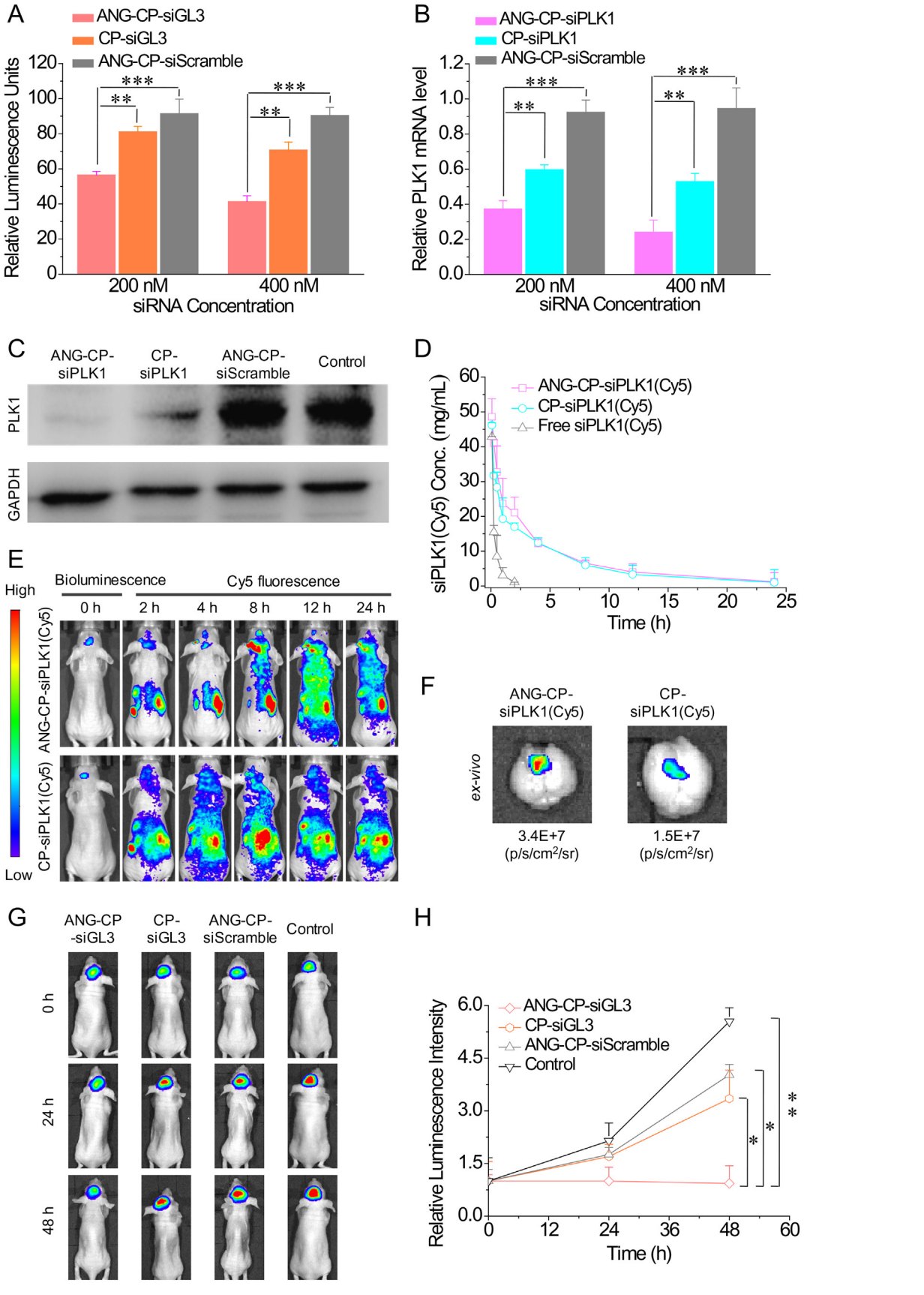

(caption on next page)

Fig. 2. A) Gene silencing potency of ANG-CP-siGL3, CP-siGL3 and ANG-CP-siScramble in U-87 MG-Luc cells after 48 h transfection (dosage: 200 or 400 nM siGL3); B) Gene silencing ability of ANG-CP-siPLK1 in U-87 MG-Luc cells after 48 h transfection (dosage: 200 or 400 nM siPLK1); C) Protein silencing ability of ANG-CP-siPLK1 in U-87 MG-Luc cells after 48 h transfection (dosage: 200 or 400 nM siPLK1); D) *In vivo* pharmacokinetics of ANG-CP-siPLK1(Cy5), CP-siPLK1(Cy5) and free siPLK1(Cy5). siPLK1(Cy5) was quantified by fluorescence spectroscopy ($n = 3$); E) The fluorescence imaging of orthotopic U-87 MG-Luc brain tumor xenografts post-injection of either ANG-CP-siPLK1(Cy5) or CP-siPLK1(Cy5). (siPLK1(Cy5) dosage: 20 μg per mouse); F) The *ex-vivo* fluorescence images of orthotopic U-87 MG-Luc brain tumor; G) *In vivo* gene silencing activity of ANG-CP-siGL3 in the orthotopic U-87 MG-Luc brain tumor-bearing nude mice. Luciferase expression of brain in the mice before and 24 or 48 h after injection of ANG-CP-siGL3, CP-siGL3 or ANG-CP-siScramble. (siRNA dosage: 60 μg/mouse); H) *Ex vivo* bioluminescence intensity of the brain tumor.

CP-siPLK1 and ANG-CP-siScramble, respectively, with similar siRNA loading, size, and surface charge (Table S1). Notably, gel retardation assays showed complete encapsulation of siRNA (siPLK1 or siScramble) into polymersomes as well as rapid siRNA release in a reductive environment containing 10 mM GSH (Fig. 1B).

The bEnd.3 monolayers and U-87 MG glioblastoma cells were cultured to evaluate *in vitro* BBB transcytosis and glioblastoma targeting of ANG-CP, respectively [42,43]. For ease of monitoring, Cy5-labeled siScramble (siScramble(Cy5)) was used as a model siRNA. The efflux ratio of ANG-CP-siScramble(Cy5) for the bEnd.3 monolayer was 1.8 at 6 h incubation and increased to 2.4 and 2.5 at 12 and 24 h incubation, respectively (Fig. 1C). In sharp contrast, both non-targeted CP-siScramble(Cy5) and free siScramble(Cy5) displayed an efflux ratio close to 1.0, *i.e.* similar apical-to-basolateral and basolateral-to-apical transportation. These results support that ANG-CP has a high BBB transcytosis likely mediated *via* LRP-1 overexpressed on bEnd.3 cells [44].

In addition to brain capillary endothelial cells, LRP-1 is also overexpressed on U-87 MG human glioblastoma cells [45]. Both BBB transcytosis and U-87 MG cellular uptake play critical roles in the efficacy of ANG-CP-siPLK1 against orthotopic glioblastoma *in vivo*. Fig. 1D shows that ANG-CP-siScramble(Cy5) exhibited a 2.5-fold better uptake after 4 h incubation by U-87 MG cells than the non-targeted CP-siScramble(Cy5), supporting LRP-1 mediated internalization of ANG-CP-siScramble(Cy5) [14,46]. Confocal microscopy displayed strong Cy5 fluorescence in the U-87 MG cells treated with ANG-CP- siScramble (Cy5), which was much stronger than that of U-87 MG cells treated with CP-siScramble(Cy5) (Fig. 1E), further corroborating that ANG-CP mediates targeted and efficient delivery of siRNA to U-87 MG cells. Endo/lysosomal escape is a key step for siRNA delivery [47,48]. Confocal images showed that while most ANG-CP-siScramble(Cy5) remains entrapped in the endosomes of U-87 MG cells at 1 and 2 h incubation, a significant amount of ANG-CP-siScramble(Cy5) has escaped from the endosomes following 4 h incubation (Fig. 1F).

3.2. In vitro and in vivo gene silencing efficacy of siRNA-loaded ANG-CP

The *in vitro* gene silencing efficacy of ANG-CP was evaluated using either siGL3 or siPLK1 in U-87 MG-Luc cells. Luminescence analysis demonstrated clearly that ANG-CP-siGL3 at 200 nM siGL3 equiv. caused effective gene silencing in U-87 MG-Luc cells, which was significantly better than CP-siGL3 (reporter luminescence down-regulation efficacy: 44% *versus* 19%, $p < 0.01$) (Fig. 2A). At an increased siGL3 dosage of 400 nM, 59% and 30% of reporter luminescence in U-87 MG-Luc cells was silenced by ANG-CP-siGL3 and CP-siGL3, respectively. In comparison, ANG-CP-siScramble induced little reporter luminescence silencing, corroborating the specific gene knockdown effect of ANG-CP-siGL3. The gene silencing efficacy of ANG-CP-siGL3 against firefly luciferase-expressing U-87 MG-Luc cells was comparable to that reported for siGL3-loaded Lipofectamine2000 in prostate cancer cells [49]. MTT assays revealed that empty ANG-CP and CP had little toxicity against U-87 MG cells at a polymersome concentration of 1 mg/mL (Fig. S2).

We then evaluated the *in vitro* silencing efficacy of ANG-CP-siPLK1 for the target oncogene PLK1 by quantifying the PLK1 mRNA level in U-87 MG-Luc cells. Fig. 2B shows that the relative PLK1 expression levels of U-87 MG-Luc cells treated with ANG-CP-siPLK1 were significantly lower than those with CP-siPLK1 (37% *versus* 59% at 200 nM and 24% *versus* 53% at 400 nM, respectively, $p < 0.01$). Western blot analysis confirmed that U-87 MG-Luc cells after treatment with ANG-CP-siPLK1 had a remarkably low PLK1 oncoprotein level (Fig. 2C). The non-targeted CP-siPLK1 also caused significant reduction of PLK1. Quantitative analysis of the western blot results indicated 89% and 67% decrease of PLK1 oncoprotein expression in U-87 MG-Luc cells treated with ANG-CP-siPLK1 and CP-siPLK1, respectively. No silencing effect was observed for ANG-CP-siScramble. The superior gene silencing efficacy of ANG-CP-siPLK1 corroborates efficient internalization of ANG-CP-siPLK1 by U-87 MG-Luc cells and fast cytoplasmic release of siPLK1.

For pharmacokinetic studies, tumor-free mice were *i.v.* injected with ANG-CP-siPLK1(Cy5) (20 μg siPLK1(Cy5) equiv./animal) and siPLK1(Cy5) was monitored at different time points. Interestingly, ANG-CP-siPLK1(Cy5) displayed a long plasma half-life ($t_{1/2\beta}$) of 4.3 h, similar to that of CP-siPLK1(Cy5) (Fig. 2D), indicating that the presence of the ANG peptide does not have much influence on the pharmacokinetics of polymersomal siRNA [50]. In contrast, free siPLK1(Cy5) was quickly eliminated from the circulation ($t_{1/2\beta} = 0.36$ h).

The accumulation of ANG-CP-siPLK1(Cy5) in orthotopic U-87 MG-Luc glioblastoma was monitored by real-time near infrared fluorescence imaging. The intracranial tumor was easily discerned by the bioluminescence of the luciferase reporter gene (Fig. 2E). Notably, ANG-CP-siPLK1(Cy5) was clearly observed at the glioblastoma site at 4 h post-injection and tumor Cy5 fluorescence was strongest at 8 h post-injection. In contrast, no difference in Cy5 fluorescence could be detected between the tumor site and surrounding area for mice administered with CP-siPLK1(Cy5) throughout the 24 h post-injection period. The *ex-vivo* imaging revealed a 2.3-fold stronger Cy5 fluorescence in glioblastoma of mice treated with ANG-CP-siPLK1(Cy5) than that with non-targeted CP-siPLK1(Cy5) counterpart (Fig. 2F). More importantly, ANG-CP-siPLK1(Cy5) was found to accumulate in the tumor site, but not in the brain parenchyma, indicating that ANG-CP-siPLK1(Cy5) selectively penetrates the blood brain tumor barrier (BBTB) owing to the specific overexpression of LRP-1 in the neovasculature in the tumor lesion [51]. In comparison, many brain targeting systems were shown to deliver cargos to both tumor lesions and brain parenchyma [52,53]. The accumulation of CP-siPLK1(Cy5) in glioblastoma was most probably due to the EPR effect, which increases along with the development of glioblastoma [54].

The gene silencing activity of ANG-CP-siGL3 was further evaluated on orthotopically xenografted U-87 MG-Luc glioblastoma in nude mice. Fig. 2G shows that in contrast to rapid increase of glioblastoma bioluminescence in mice treated with CP-siGL3 and ANG-CP-siScramble, little change in glioblastoma bioluminescence was observed for the ANG-CP-siGL3 group. The glioblastoma bioluminescence was significantly lower in mice treated with ANG-CP-siGL3 than with CP-siGL3 or ANG-CP-siScramble (Fig. 2H), confirming that ANG-CP-siGL3 can effectively interfere with the expression of the luciferase reporter gene *in vivo*.

3.3. Anti-glioblastoma effect of ANG-CP-siPLK1

The anti-glioblastoma effect of ANG-CP-siPLK1 was studied in orthotopically xenografted U-87 MG-Luc tumors at a dose of 60 μg siPLK1. The results showed that ANG-CP-siPLK1 potently retarded the development of glioblastoma compared with the non-targeted CP-siPLK1 and

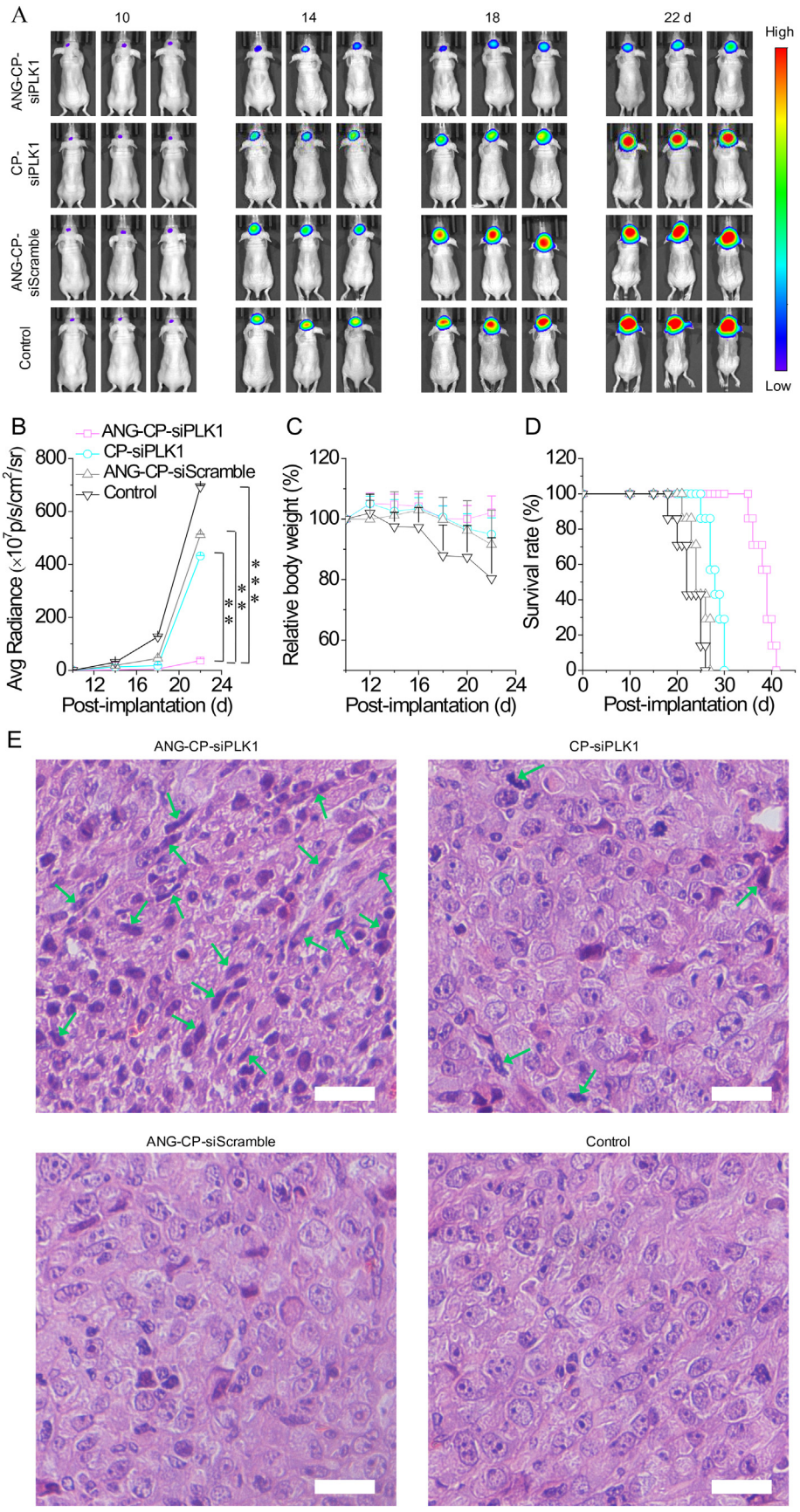

Fig. 3. A) Luminescence optical images of orthotopic U-87-Luc brain tumor-bearing nude mice following treatment with ANG-CP-siPLK1, CP-siPLK1, ANG-CP-siScramble, and PBS (control). The mice were intravenously injected at a dose of 60 μg siPLK1 or siScramble per mouse on day 10, 12, 14, 16 and 18; B) Quantified luminescence levels of mice using the Lumina IVIS II system; C) Relative body weight changes of mice; D) Kaplan–Meier survival curve of mice; E) Histological analyses of tumors excised from orthotopic U-87-Luc glioblastoma-bearing nude mice on day 20. The arrows in the images indicated the condensation of chromatin of glioblastoma cells. The images were obtained with an Olympus BX41 microscope. Bar: 50 μm.

placebo controls (Fig. 3A). The quantification of tumor bioluminescence revealed significantly better inhibition of tumor growth by ANG-CP-siPLK1 than CP-siPLK1 and ANG-CP-siScramble (Fig. 3B). Fig. 3C displays that body weights of mice treated with CP-siPLK1, ANG-CP-siScramble or PBS decreased as a result of glioblastoma progression and brain disorder. In contrast, ANG-CP-siPLK1 group exhibited no reduction of body weight, confirming that ANG-CP-siPLK1 can effectively retard tumor invasion and has low side effects. Furthermore, Kaplan–Meier survival curves showed that ANG-CP-siPLK1 greatly extended the lifespan of mice compared with CP-siPLK1, ANG-CP-siScramble and PBS (median survival time: 39 *versus* 27, 24 and 22 days, respectively) (Fig. 3D). Morphological nuclear changes, mainly chromatin condensation and nuclear fragmentation, are hallmarks of apoptosis of cancer cells [55,56]. Previous studies also reported that the silencing of PLK1 will result in the inactivation of cyclin-dependent kinase 1 and mitotic arrest, followed by apoptosis [57]. Severe chromatin condensation in excised U-87 MG glioblastoma sections from the animal with ANG-CP-siPLK1 therapy shown by H&E staining confirmed pronounced antitumor effect of ANG-CP-siPLK1 (Fig. 3E). In comparison, chromatin condensation of glioblastoma cells occurred to a less extent in CP-siPLK1 group, and hardly observed in animals treated with ANG-CP-siScramble or PBS. In addition, no obvious tissue damage was found in the H&E staining of normal organs (including heart, liver, spleen, lung and kidney), indicating excellent bio-safety of our polymersomal siRNA (Fig. S3). This is in sharp contrast to anti-glioblastoma nanosystems based on chemotherapeutics that were shown to cause significant non-specific toxicity [18,58]. Hence, ANG-CP-siPLK1 is able to penetrate BBB and induce potent and targeted gene silencing of glioblastoma *in vivo*.

4. Conclusions

The results at hand highlight that angiopep-2-decorated chimaeric polymersomes are a simple, nontoxic and brain-targeting non-viral vector that boosts the RNAi therapy for human glioblastoma *in vivo*. These brain-targeting polymersomes uniquely integrate all functions in one: (i) they show excellent packaging and protection of siPLK1 in the watery core; (ii) they greatly prolong the siRNA circulation time; (iii) they can not only effectively permeate blood-brain barrier but also actively target to glioblastoma cells, *via* the LRP-1 mediated pathway; (iv) they significantly enhance siRNA accumulation in glioblastoma, and (v) after internalization by glioblastoma cells, they quickly dissociate and release siRNA into cytosols, leading to effective gene silencing. The therapeutic results using siPLK1 and U-87 MG orthotopic glioblastoma as model siRNA and brain tumor, respectively, prove the concept that these multifunctional polymersomes can boost brain-targeted RNAi therapy.

Acknowledgements

This work was supported by the National Natural Science Foundation of China (NSFC 51403147, 51561135010, 51633005, 51761135117).

Appendix A. Supplementary data

Supplementary data to this article can be found online at https://doi.org/10.1016/j.jconrel.2018.10.034.

References

[1] A. Omuro, L.M. Deangelis, Glioblastoma and other malignant gliomas a clinical review, JAMA 310 (2013) 1842–1850.
[2] B. Obermeier, R. Daneman, R.M. Ransohoff, Development, maintenance and disruption of the blood-brain barrier, Nat. Med. 19 (2013) 1584–1596.
[3] A. Carpentier, M. Canney, A. Vignot, V. Reina, K. Beccaria, C. Horodyckid, et al., Clinical trial of blood-brain barrier disruption by pulsed ultrasound, Sci. Transl. Med. 8 (2016) 343re2.
[4] W.A. Banks, From blood-brain barrier to blood-brain interface: new opportunities for CNS drug delivery, Nat. Rev. Drug Discov. 15 (2016) 275–292.
[5] T.F. Cloughesy, W.K. Cavenee, P.S. Mischel, Glioblastoma: from molecular pathology to targeted treatment, Annu. Rev. Pathol. 9 (2014) 1–25.
[6] B. Oller-Salvia, M. Sanchez-Navarro, E. Giralt, M. Teixido, Blood-brain barrier shuttle peptides: an emerging paradigm for brain delivery, Chem. Soc. Rev. 47 (2016) 4690–4707.
[7] A.A. Thomas, C.W. Brennan, L.M. Deangelis, A.M. Omuro, Emerging therapies for glioblastoma, Jama Neurol. 71 (2014) 1437–1444.
[8] E.G. van Meir, C.G. Hadjipanayis, A.D. Norden, H.K. Shu, P.Y. Wen, J.J. Olson, Exciting new advances in neuro-oncology: the avenue to a cure for malignant glioma, CA Cancer J. Clin. 60 (2010) 166–1693.
[9] S.L. Gonias, W.M. Campana, LDL receptor-related protein-1: a regulator of inflammation in atherosclerosis, cancer, and injury to the nervous system, Am. J. Pathol. 184 (2014) 18–27.
[10] S.E. Storck, S. Meister, J. Nahrath, J.N. Meißner, N. Schubert, S.A. Di, et al., Endothelial LRP1 transports amyloid-β_{1-42} across the blood-brain barrier, J. Clin. Invest. 126 (2016) 123–136.
[11] D. Ni, J. Zhang, W. Bu, H. Xing, F. Han, Q. Xiao, Z. Yao, et al., Dual-targeting upconversion nanoprobes across the blood-brain barrier for magnetic resonance/fluorescence imaging of intracranial glioblastoma, ACS Nano 8 (2014) 1231–1242.
[12] M. Demeule, J.C. Currie, Y. Bertrand, C. Che, T. Nguyen, A. Regina, et al., Involvement of the low-density lipoprotein receptor-related protein in the transcytosis of the brain delivery vector angiopep-2, J. Neurochem. 106 (2008) 1534–1544.
[13] J.S. Kim, D.H. Shin, J.S. Kim, Dual-targeting immunoliposomes using angiopep-2 and CD133 antibody for glioblastoma stem cells, J. Control. Release 269 (2018) 245–257.
[14] X. Ying, Y. Wang, J. Liang, J. Yue, C. Xu, L. Lu, et al., Angiopep-conjugated electroresponsive hydrogel nanoparticles: therapeutic potential for epilepsy, Angew. Chem. 53 (2014) 12436–12440.
[15] Y. Zhu, Y. Jiang, F. Meng, C. Deng, R. Cheng, J. Zhang, et al., Highly efficacious and specific anti-glioma chemotherapy by tandem nanomicelles co-functionalized with brain tumor-targeting and cell-penetrating peptides, J. Control. Release 278 (2018) 1–8.
[16] J. Drappatz, A. Brenner, E.T. Wong, A. Eichler, D. Schiff, M.D. Groves, et al., Phase I study of GRN1005 in recurrent malignant glioma, Clin. Cancer Res. 19 (2013) 1567–1576.
[17] A. Regina, M. Demeule, S. Tripathy, S. Lorddufour, J.C. Currie, M. Iddir, et al., ANG4043, a novel brain-penetrant peptide-mAb conjugate, is efficacious against HER2-positive intracranial tumors in mice, Mol. Cancer Ther. 14 (2015) 129–140.
[18] S. Ruan, M. Yuan, L. Zhang, G. Hu, J. Chen, X. Cun, et al., Tumor microenvironment sensitive doxorubicin delivery and release to glioma using angiopep-2 decorated gold nanoparticles, Biomaterials 37 (2015) 425–435.
[19] H. Xin, X. Sha, X. Jiang, W. Zhang, L. Chen, X. Fang, Anti-glioblastoma efficacy and safety of paclitaxel-loading Angiopep-conjugated dual targeting PEG-PCL nanoparticles, Biomaterials 33 (2012) 8167–8176.
[20] G. Ozcan, B. Ozpolat, R.L. Coleman, A.K. Sood, G. Lopezberestein, Preclinical and clinical development of siRNA-based therapeutics, Adv. Drug Deliv. Rev. 87 (2015) 108–119.
[21] R. Kanasty, J.R. Dorkin, A. Vegas, D. Anderson, Delivery materials for siRNA therapeutics, Nat. Mater. 12 (2013) 967–977.
[22] K.L. Kozielski, S.Y. Tzeng, B.A.H.D. Mendoza, J.J. Green, Bioreducible cationic polymer-based nanoparticles for efficient and environmentally triggered cytoplasmic siRNA delivery to primary human brain cancer cells, ACS Nano 8 (2014) 3232–3241.
[23] J.E. Zuckerman, M.E. Davis, Clinical experiences with systemically administered siRNA-based therapeutics in cancer, Nat. Rev. Drug Discov. 14 (2015) 843–856.
[24] A. Wittrup, J. Lieberman, Knocking down disease: a progress report on siRNA therapeutics, Nat. Rev. Genet. 16 (2015) 543–552.
[25] R.C. Wilson, J.A. Doudna, Molecular mechanisms of RNA interference, Annu. Rev. Biophys. 42 (2013) 217–239.
[26] Z.R. Cohen, S. Ramishetti, N. Peshes-Yaloz, M. Goldsmith, A. Wohl, Z. Zibly, et al., Localized RNAi therapeutics of chemoresistant grade IV glioma using hyaluronan-grafted lipid- based nanoparticles, ACS Nano 9 (2015) 1581–1591.
[27] R.G. Lerner, S. Grossauer, B. Kadkhodaei, I. Meyers, M. Sidorov, K. Koeck, et al., Targeting a Plk1-controlled polarity checkpoint in therapy-resistant glioblastoma-propagating cells, Cancer Res. 75 (2015) 5355–5366.
[28] N. Pozo, C. Zahonero, P. Fernandez, J.M. Linares, A. Ayuso, M. Hagiwara, et al., Inhibition of DYRK1A destabilizes EGFR and reduces EGFR-dependent glioblastoma growth, J. Clin. Invest. 123 (2013) 2475–2487.
[29] R.G. Verhaak, K.A. Hoadley, E. Purdom, V. Wang, Y. Qi, M.D. Wilkerson, et al., Integrated genomic analysis identifies clinically relevant subtypes of glioblastoma characterized by abnormalities in PDGFRA, IDH1, EGFR, and NF1, Cancer Cell 17 (2010) 98–110.
[30] S.A. Jensen, E.S. Day, C.H. Ko, L.A. Hurley, J.P. Luciano, F.M. Kouri, et al., Spherical nucleic acid nanoparticle conjugates as an RNAi-based therapy for glioblastoma, Sci. Transl. Med. 5 (2013) 209ra152.
[31] J.L. Huang, G. Jiang, Q.X. Song, X. Gu, M. Hu, X.L. Wang, et al., Lipoprotein-biomimetic nanostructure enables efficient targeting delivery of siRNA to Ras-activated glioblastoma cells via macropinocytosis, Nat. Commun. 8 (2017) 15144–15161.
[32] M. van Woensel, N. Wauthoz, R. Rosiere, V. Mathieu, R. Kiss, F. Lefranc, et al., Development of siRNA-loaded chitosan nanoparticles targeting Galectin-1 for the treatment of glioblastoma multiforme via intranasal administration, J. Control. Release 227 (2016) 71–81.

[33] D. Yu, O.F. Khan, M.L. Suva, B. Dong, W.K. Panek, T. Xiao, et al., Multiplexed RNAi therapy against brain tumor-initiating cells via lipopolymeric nanoparticle infusion delays glioblastoma progression, Proc. Natl. Acad. Sci. U. S. A. 114 (2017) E6147–E6156.
[34] Y. Zou, M. Zheng, W. Yang, F. Meng, K. Miyata, H.J. Kim, et al., Virus-mimicking chimaeric polymersomes boost targeted cancer siRNA therapy in vivo, Adv. Mater. 29 (2017) 1603997.
[35] H. Xin, X. Jiang, J. Gu, X. Sha, L. Chen, K. Law, et al., Angiopep-conjugated poly (ethylene glycol)-co-poly(epsilon-caprolactone) nanoparticles as dual-targeting drug delivery system for brain glioma, Biomaterials 32 (2011) 4293–4305.
[36] X. Jiang, H. Xin, Q. Ren, J. Gu, L. Zhu, F. Du, et al., Nanoparticles of 2-deoxy-D-glucose functionalized poly(ethylene glycol)-co-poly(trimethylene carbonate) for dual-targeted drug delivery in glioma treatment, Biomaterials 35 (2014) 518–529.
[37] D.E. Zak, A. Penn-Nicholson, T.J. Scriba, E. Thompson, S. Suliman, L.M. Amon, et al., A blood RNA signature for tuberculosis disease risk: a prospective cohort study, Lancet 387 (2016) 2312–2322.
[38] C.C. Kang, K.A. Yamauchi, J. Vlassakis, E. Sinkala, T.A. Duncombe, A.E. Herr, Single cell–resolution western blotting, Nat. Protoc. 11 (2016) 1508–1530.
[39] H. Yin, R.L. Kanasty, A.A. Eltoukhy, A.J. Vegas, J.R. Dorkin, D.G. Anderson, Non-viral vectors for gene-based therapy, Nat. Rev. Genet. 15 (2014) 541–555.
[40] U. Lachelt, E. Wagner, Nucleic acid therapeutics using polyplexes: a journey of 50 years (and beyond), Chem. Rev. 115 (2015) 11043–11078.
[41] H. Wei, L.R. Volpatti, D.L. Sellers, D.O. Maris, I.W. Andrews, A.S. Hemphill, et al., Dual responsive, stabilized nanoparticles for efficient in vivo plasmid delivery, Angew. Chem. 52 (2013) 5377–5381.
[42] T.J. Yuen, J.C. Silbereis, A. Griveau, S.M. Chang, R. Daneman, S.P.J. Fancy, et al., Oligodendrocyte-encoded HIF function couples postnatal myelination and white matter angiogenesis, Cell 158 (2014) 383–396.
[43] B.J. Andreone, B.W. Chow, A. Tata, B. Lacoste, A. Ben-Zvi, K. Bullock, et al., Blood-brain barrier permeability is regulated by lipid transport-dependent suppression of caveolae-mediated transcytosis, Neuron 94 (2017) 581–594.
[44] R. Deane, Z. Wu, A. Sagare, J. Davis, S.D. Yan, K. Hamm, et al., LRP/Amyloid β-peptide interaction mediates differential brain efflux of Aβ isoforms, Neuron 43 (2004) 333–344.
[45] K. Boyé, N. Pujol, I.D. Alves, Y.P. Chen, T. Daubon, Y.Z. Lee, et al., The role of CXCR3/LRP1 cross-talk in the invasion of primary brain tumors, Nat. Commun. 8 (2017) 1571–1590.
[46] J. Chen, X. Cun, S. Ruan, Y. Wang, Y. Zhang, Q. He, et al., Glioma cell-targeting doxorubicin delivery and redox-responsive release using angiopep-2 decorated carbonaceous nanodots, RSC Adv. 5 (2015) 57045–57049.
[47] J. Gilleron, W. Querbes, A. Zeigerer, A. Borodovsky, G. Marsico, U. Schubert, et al., Image-based analysis of lipid nanoparticle-mediated siRNA delivery, intracellular trafficking and endosomal escape, Nat. Biotechnol. 31 (2013) 638–646.
[48] T.F. Martens, K. Remaut, J. Demeester, S.C.D. Smedt, K. Braeckmans, Intracellular delivery of nanomaterials: how to catch endosomal escape in the act, Nano Today 9 (2014) 344–364.
[49] G. Pisignano, S. Napoli, M. Magistri, S.N. Mapelli, C. Pastori, S. Di Marco, et al., A promoter-proximal transcript targeted by genetic polymorphism controls E-cadherin silencing in human cancers, Nat. Commun. 8 (2017) 15622.
[50] Y. Hao, B. Zhang, C. Zheng, R. Ji, X. Ren, F. Guo, et al., The tumor-targeting core-shell structured DTX-loaded PLGA@Au nanoparticles for chemo-photothermal therapy and X-ray imaging, J. Control. Release 220 ((2015) 545–555.
[51] D. Alan, Breaching the barrier, Nat. Biotechnol. 26 (2008) 1213–1216.
[52] Y. Qian, Y. Zha, B. Feng, Z. Pang, B. Zhang, X. Sun, et al., PEGylated poly(2-(dimethylamino) ethyl methacrylate)/DNA polyplex micelles decorated with phage-displayed TGN peptide for brain-targeted gene delivery, Biomaterials 34 (2013) 2117–2129.
[53] Z.R. Stephen, F.M. Kievit, O. Veiseh, P.A. Chiarelli, C. Fang, K. Wang, et al., Redox-responsive magnetic nanoparticle for targeted convection-enhanced delivery of O6-Benzylguanine to brain tumors, ACS Nano 8 (2014) 10383–10395.
[54] H. Wolburg, S. Noell, P. Fallier-Becker, A.F. Mack, K. Wolburg-Buchholz, The disturbed blood-brain barrier in human glioblastoma, Mol. Asp. Med. 33 (2012) 579–589.
[55] S. Sahara, M. Aoto, Y. Eguchi, N. Imamoto, Y. Yoneda, Y. Tsujimoto, Acinus is a caspase-3-activated protein required for apoptotic chromatin condensation, Nature 401 (1999) 168–173.
[56] Z. Lu, C. Zhang, Z. Zhai, Nucleoplasmin regulates chromatin condensation during apoptosis, Proc. Natl. Acad. Sci. U. S. A. 102 (2005) 2778–2783.
[57] S. Reagan-Shaw, N. Ahmad, Silencing of polo-like kinase (Plk) 1 via siRNA causes induction of apoptosis and impairment of mitosis machinery in human prostate cancer cells: implications for the treatment of prostate cancer, FASEB J. 19 (2005) 611.
[58] Z.Z. Yang, J.Q. Li, Z.Z. Wang, D.W. Dong, X.R. Qi, Tumor-targeting dual peptides-modified cationic liposomes for delivery of siRNA and docetaxel to gliomas, Biomaterials 35 (2014) 5226–5239.